Off–Resonance TROSY (R 1 ρ − R 1) for Quantitation of Fast Exchange Processes in Large Proteins

4 AUTHORS, INCLUDING:

Nicole Sampson
Stony Brook University

96 PUBLICATIONS   **2,422** CITATIONS

Off-Resonance TROSY ($R_{1\rho} - R_1$) for Quantitation of Fast Exchange Processes in Large Proteins

James G. Kempf,[§] Ju-yeon Jung,[†] Nicole S. Sampson,[†] and J. Patrick Loria*,[§]

Department of Chemistry, Yale University, P.O. Box 208107, New Haven, Connecticut 06520, and Department of Chemistry, State University of New York, Stony Brook, New York 11794-3400

Received July 7, 2003; E-mail: patrick.loria@yale.edu

Elucidating the physicochemical details of functionally important macromolecular dynamics is an important goal in chemistry and biology. Nuclear magnetic resonance (NMR) is the perhaps the most versatile and powerful tool applied to this problem[1,2] but is impeded by two important obstacles: the difficulty of obtaining high-quality spectra as molecular size increases and the narrow time scale to which a given NMR experiment is limited for sensing molecular motion. Major progress has been made in these areas to aid characterization of conformational exchange in small proteins via NMR spin-relaxation experiments.[3,4] However, the majority of natural proteins contain more than 200 amino acids and, with corresponding structural variety, may be expected to exhibit dynamics over a broad range of time scales. Current experiments to quantitate exchange in large proteins are limited to motion at time scales ≥ 300 μs,[2,5] yet many biological processes are more rapid than this value.[4,6]

Here, we present a solution NMR experiment that quantifies conformational exchange rates to time scales at least an order of magnitude faster than previously possible for large proteins and demonstrate the method on a 53-kDa protein (24 ns tumbling time at 293 K). The new experiment utilizes ^{15}N relaxation in the presence of an off-resonance spin-lock field to access μs to ms dynamics,[4] while incorporating transverse relaxation optimized (TROSY) coherence selection[7] in both ^{1}H and ^{15}N dimensions to enable study of large systems. Adiabatic amplitude and frequency sweeps of the rf field optimally align ^{15}N magnetization at all sites in the molecule with the spin-lock field,[8] while state-of-the-art broadband ^{1}H decoupling is achieved using the random-phase alternation (RPA) scheme.[9] Finally, the constant-time design of the relaxation yields decay at the difference ($R_{1\rho} - R_1$) between spin-locked and longitudinal rates, reducing parametrization for the ultimate quantification of exchange.[4]

Two-site, fast conformational exchange in the presence of an off resonance spin-lock field yields[10]

$$R_{1\rho} = R_1 \cos^2 \theta + R_2 \sin^2 \theta + \frac{p_A p_B \, \Delta\omega^2 k_{ex} \sin^2 \theta}{k_{ex}^2 + \omega_e^2} \quad (1)$$

where $R_2(R_1)$ is the transverse(longitudinal) spin-relaxation rate, $\theta = \tan^{-1}(\omega_1/\Delta\Omega)$ is the angle of the spin-lock field with respect to the static field, while ω_1 and $\Delta\Omega$ are, respectively, the rf amplitude and frequency offset from the population-weighted average chemical shift of the two conformers. The last term in eq 1 contains the exchange contribution to spin relaxation:

$$R_{ex} = \frac{p_A p_B \Delta\omega^2 k_{ex}}{k_{ex}^2 + \omega_e^2} \quad (2)$$

[§] Yale University.
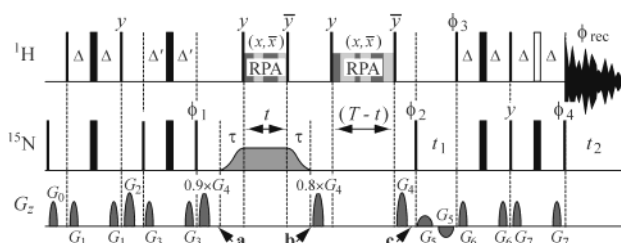[†] State University of New York at Stony Brook.

Figure 1. TROSY ($R_{1\rho} - R_1$) pulse sequence for exchange characterization at ^{15}N sites. TROSY selection in t_1 and t_2 and PEP[11] coherence modulation are achieved with a phase cycle yielding an echo signal for ϕ_1 = 4y, 4($-y$), $\phi_2 = y, -y, -x, x, -y, y, x, -x$; $\phi_3 = y$, $\phi_4 = x$ and ϕ_{rec} = $x, -x, y, -y$, and the anti-echo counterpart with inversion of ϕ_3 and ϕ_4 and replacement of ϕ_{rec} with $-x, x, y, -y$. In each case, ϕ_2 and ϕ_{rec} are inverted on alternate steps in t_1. Phases are specific to Varian spectrometers. CSA/dipolar suppression[12] during T is achieved with random phase variation, x to $-x$, occurring at 10 ms average interval and employing a distinct random pattern on each transient of each t_1 increment. A 5.8 kHz amplitude decoupling field is typical. Gradient magnitudes $G_0 - G_7$ are 8.7, 10.8, 32.5, 11.9, 39.0, 1.5, 13.0, and 17.4 G/cm with durations 1.0, 0.6, 0.9, 0.6, 1.5, 1.0, 0.6, and 0.6 ms. The bipolar pair, G_5, is set sufficient to dephase ^{1}H$_2$O for suppression of radiation damping although is omitted entirely when $t_1 < 800$ μs, and applied for 0.4 ms when 0.8 ms $\leq t_1 \leq$ 2.0 ms. Delays are Δ, $\Delta' = 2.7$, 2.5 ms, and $\tau = 4$ ms. The open bar on the ^{1}H timeline represents the 3$-$9$-$19 selective pulse element.[13] Finally, rf influence on sample temperature is rendered t-independent by irradiating ^{15}N at the spin-lock power level off-resonance during the 2.5 s recycle delay (not shown).

where $p_{A(B)}$ are the equilibrium populations of exchanging sites A and B, differing by $\Delta\omega$ in chemical shift, the exchange rate, k_{ex}, is the sum of forward and reverse rates, and $\omega_e = (\omega_1/\sin \theta) = (\Delta\Omega /\cos \theta)$ is the strength of the effective rotating-frame spin-lock field. The fast limit used to derive eqs 1 and 2 requires $k_{ex} \gg \Delta\omega$.

Quantifying motional processes is simplified here relative to experiments governed by eq 1, as constant-time relaxation yields an effective spin-relaxation rate,[4]

$$R_{eff} = (R_{1\rho} - R_1) = (R_2 - R_1) \sin^2 \theta + R_{ex} \sin^2 \theta \quad (3)$$

which reduces the parametrization required to extract R_{ex}. Rates determined as a function of ω_1 and/or $\Delta\Omega$ yield a series of values, R_{eff} /sin^2 θ, vs θ. In such a series, only R_{ex} varies with θ via ω_e, and fits to the sum of R_{ex} [eq 2] and the constant offset ($R_2 - R_1$) provide the exchange rate, k_{ex} and the product $p_A p_B\Delta\omega^2$, at multiple sites across the protein.

Figure 1 depicts the TROSY ($R_{1\rho} - R_1$) pulse sequence. The relaxation segment begins at point **a** on the timeline. Preceding INEPT transfers prepare pure ^{15}N coherence in either $\pm S_z$ longitudinal states. At **a**, the ^{15}N carrier is moved to the desired off-resonance value, while that of the ^{1}H is moved to the amide center. Adiabatic rotation of $\pm S_z$ to the effective field at θ is achieved by the use of amplitude and frequency sweeps over time τ, with tanh and tan modulation,[8] respectively. Spin-locked coherence then relaxes at rate $R_{1\rho}$ for time t, after which it is returned to the z axis
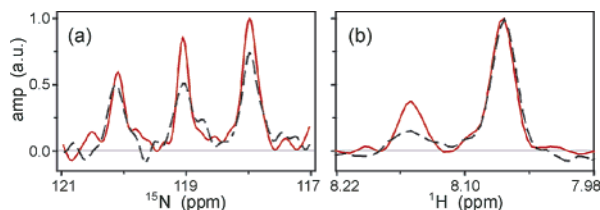
Figure 2. Slices along (a) ^{15}N and (b) ^{1}H comparing TROSY (solid, red) and conventional (dashed, black) experiments for $(R_{1\rho} - R_1)$. Spectra were collected with 16 scans, $t = 20$ ms, $T = 160$ ms, $\omega_1 = 1.02 \pm 0.14$ kHz applied at 86.1 ppm and calibrated as described.[1] Acquisition included 180 t_1 and 2304 t_2 points and 2.4 kHz and 12 kHz spectral width. Non-TROSY profiles are shifted by $(J_{NH}/2)$ to align the spectra for easy comparison. The sample and apparatus used are detailed in the text.

at **b** by reversal of the first adiabatic sweep. During t, CSA/dipolar cross-relaxation is suppressed with the RPA decoupling scheme.[9] The ^{1}H bandwidth of RPA exceeds that of constant interval phase alternation by an amount that is significant in very high field (≥ 800 MHz) application, which is always desirable, and often necessary, with large proteins. Following **b**, RPA-decoupled longitudinal relaxation for $(T - t)$ at rate R_1 completes the constant-time period with aggregate, effective decay at $(R_{1\rho} - R_1)$. RPA periods are bracketed by ^{1}H $\pi/2$ pulses to return ^{1}H$_2$O magnetization to a consistent orientation independent of the random sequence, while gradients in multiples of G_4 dephase any residual transverse coherence. At **c**, the rf carriers are returned to ^{1}H$_2$O and the ^{15}N amide center.

Sensitivity-enhanced TROSY selection[7,14] is achieved in both the t_1 and t_2 periods using an eight-step phase cycle given in the caption to Figure 1. Each half cycle is a four-step sequence for complete TROSY selection. The halves differ in the sign of S_z followed through the preceding relaxation periods and are combined so that the nonvanishing ^{15}N steady state provided by the ^{1}H$-^{15}$N NOE is subtracted from the decay without perturbing TROSY selection. The same is possible with previous longer phase cycles, but this reduced step count requires half the experiment time, particularly attractive when sensitivity is abundant, as with the increasingly available cold-probe technology.

The performance of this pulse sequence is demonstrated on an 0.8 mM ^{2}H(98%),^{15}N-labeled sample of the 53-kDa enzyme, chicken triosephosphate isomerase (TIM) at 14.1 T and 293 K. Figure 2 compares signal-to-noise (S/N) and resolution from the TROSY-based experiment with a non-TROSY version.[4] Dramatic S/N increases of up to 60% and line width reductions by up to 50% are apparent from fits to these 1D slices. The average S/N increase among residues in TIM is 49 ± 16%. Additional enhancements will occur at higher fields.

Figure 3a shows relaxation decays for two residues at opposite extrema of the ^{15}N chemical shift range, and thus with greatly distinct values of θ and R_{eff}. Figure 3b plots R_{eff} for all quantifiable nonproline residues in TIM vs their corresponding θ values at $\omega_1 \sim 1$ kHz. The variation of R_{eff} among these sites matches the prediction of eq 3, and fitting the data set to $(R_2 - R_1) \sin^2 \theta$ yields the average $(R_2 - R_1) = 38.6 \pm 0.8$ s^{-1}. Anomalously low rates are likely due to rapidly reorienting sites near or at the termini of TIM. Elevated values can indicate exchange ($R_{ex} > 0$) in the μs to ms regime. The latter is quantified at each site by additionally determining R_{eff} at several values of θ,[10] as discussed above.

In conclusion, we provide an NMR experiment to characterize conformational exchange in large biological macromolecules. We

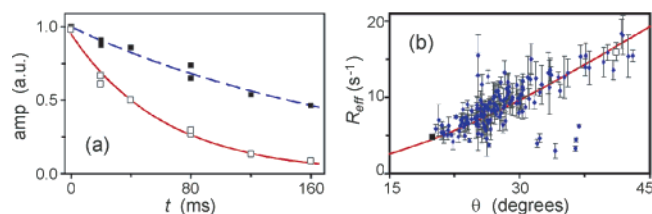**Figure 3.** (a) ^{15}N relaxation decays for amides at extremes of the ^{15}N spectral width obtained with the sequence of Figure 1, the parameters detailed in Figure 2 and the series $t = 0$, 20(2×), 40, 80(2×), 120, and 160 ms, requiring 36 h in total. Corresponding rates $(R_{1\rho} - R_1) = 4.8 \pm 0.4$ s^{-1} (■, $\theta = 20.0°$) and 16.0 ± 1.2 s^{-1} (□, $\theta = 41.2°$) appear with matching symbols in (b). There, variation of R_{eff} with θ is shown for all sites along with the fit of the full set to $(R_2 - R_1) \sin^2 \theta$. Note that θ must be calculated using the non-TROSY peak position.

have demonstrated exceptional sensitivity and resolution enhancements in the context of a state-of-the-art experiment for conformational-exchange characterization up to time scales at least an order of magnitude greater than previously accessible for large systems. These gains occurred at a relatively modest 600-MHz field and for a challenging molecular weight of 53 kDa. We employed, without sacrifice, a minimum phase cycle with an eye to increasingly available high-sensitivity cold-probe systems. This experiment should find general utility in studies of protein dynamics. The pulse sequence and details for implementation of RPA and adiabatic alignment schemes are available from http://xbeams.chem.yale.edu/~loria.

References

(1) Palmer, A. G.; Kroenke, C. D.; Loria, J. P. *Methods Enzymol.* **2001**, *339 Part B*, 204−238.
(2) Kempf, J. G.; Loria, J. P. *Cell Biochem. Biophys.* **2003**, *37*, 187−212.
(3) Szyperski, T.; Luginbühl, P.; Otting, G.; Güntert, P.; Wüthrich, K. *J. Biomol. NMR* **1993**, *3*, 151−164; Loria, J. P.; Rance, M.; Palmer, A. G. *J. Am. Chem. Soc.* **1999**, *121*, 2331−2332; Ishima, R.; Wingfield, P. T.; Stahl, S. J.; Kaufman, J. D.; Torchia, D. A. *J. Am. Chem. Soc.* **1998**, *120*, 10534−10542; Mulder, F. A.; Mittermaier, A.; Hon, B.; Dahlquist, F. W.; Kay, L. E. *Nat. Struct. Biol.* **2001**, *8*, 932−935.
(4) Akke, M.; Palmer, A. G. *J. Am. Chem. Soc.* **1996**, *118*, 911−912.
(5) Loria, J. P.; Rance, M.; Palmer, A. G. *J. Biomol. NMR* **1999**, *15*, 151−155; Zhu, G.; Xia, Y.; Nicholson, L. K.; Sze, K. H. *J. Magn. Reson.* **2000**, *143*, 423−426; Caffrey, M.; Kaufman, J.; Stahl, S.; Wingfield, P.; Gronenborn, A.; Clore, G. *J. Magn. Reson.* **1998**, *135*, 368−372; Wang, C.; Rance, M.; Palmer, A. G. *J. Am. Chem. Soc.* **2003**, *125*, 8968−8969.
(6) Akke, M.; Liu, J.; Cavanagh, J.; Erickson, H. P.; Palmer, A. G. *Nat. Struct. Biol.* **1998**, *5*, 55−59; Vugmeyster, L.; Kroenke, C. D.; Picart, F.; Palmer, A. G.; Raleigh, D. P. *J. Am. Chem. Soc.* **2000**, *122*, 5387−5388; Eisenmesser, E. Z.; Bosco, D. A.; Akke, M.; Kern, D. *Science* **2002**, *295*, 1520−1523.
(7) Pervushin, K.; Riek, R.; Wider, G.; Wuthrich, K. *Proc. Natl. Acad. Sci. U.S.A.* **1997**, *94*, 12366−12371.
(8) Desvaux, H.; Berthault, P.; Birlirakis, N.; Goldman, M.; Piotto, M. *J. Magn. Reson., Ser. A* **1995**, *113*, 47−52; Mulder, F. A. A.; de Graaf, R. A.; Kaptein, R.; Boelens, R. *J. Magn. Reson.* **1998**, *131*, 351−357.
(9) Korzhnev, D. M.; Skyrnnikov, N. R.; Millet, O.; Torchia, D.; Kay, L. E. *J. Am. Chem. Soc.* **2002**, *124*, 10743−10753.
(10) Davis, D. G.; Perlman, M. E.; London, R. E. *J. Magn. Reson., Ser B* **1994**, *104*, 266−275.
(11) Cavanagh, J.; Rance, M. *J. Magn. Reson.* **1990**, *88*, 72−85.
(12) Palmer, A. G.; Skelton, N. J.; Chazin, W. J.; Wright, P. E.; Rance, M. *Mol. Phys.* **1992**, *75*, 699−711.
(13) Sklenar, V.; Piotto, M.; Leppik, R.; Saudek, V. *J. Magn. Reson., Ser. A* **1993**, *102*, 241−245.
(14) Rance, M.; Loria, J. P.; Palmer, A. G. *J. Magn. Reson.* **1999**, *136*, 92−101.

JA037101S